Available online at www.sciencedirect.com
SCIENCE DIRECT®
Journal of Organometallic Chemistry 667 (2003) 103–111
Journal of Organometallic Chemistry
www.elsevier.com/locate/jorganchem

Rhenium pentahydride complexes: characterisation and protonation reactions. Crystal structure of $ReH_5L^1L^2$ ($L^1 = Ph_2PO(CH_2)_2OPPh_2$; $L^2 = P(OCH_3)_3$, $P(OCH_2CH_3)_3$)

Sandra Bolaño, Jorge Bravo *, Soledad García-Fontán, Jesús Castro

Departamento de Química Inorgánica, Universidade de Vigo, Lagoas-Marcosende, E-36200 Vigo, Spain

Received 21 October 2002; received in revised form 27 November 2002; accepted 2 December 2002

Abstract

Variable temperature NMR studies of the rhenium pentahydrides $[ReH_5L^1L^2]$ ($L^1 = Ph_2POCH_2CH_2OPPh_2$; $L^2 = PPh_n(OR)_{3-n}$, $n = 0–2$; R = Me, Et) show a fluxional behaviour at all accessible temperatures. The coalescence events observed in the hydride region of the ^{1}H-NMR spectra have coalescence temperatures increasing as the number of OR groups of L^2 increases. Longitudinal $T_{1(min)}$ values (~ 120 ms at 400 MHz) suggest a classical nature for these compounds. The crystal structure of compounds with $L^2 = P(OR)_3$ has been determined by X-ray diffraction techniques at low temperature. Both compounds show a dodecahedral co-ordination geometry with the three phosphorus nuclei and one hydride in B sites and the remaining four hydrides in A sites. The protonation of pentahydrides with $HBF_4 \cdot Et_2O$ yielded the non-classical cations $[Re(\eta^2\text{-}H_2)H_4L^1L^2]^+$ ($T_{1(min)} \sim 20$ ms at 400 MHz) that slowly decompose between 253 and 273 K being more stable as the number of OR groups increases.

Keywords: Rhenium; Hydride compounds; Dihydrogen compounds; Phosphites

1. Introduction

The interest for the chemistry of hydride transition metal complexes is increasing in inorganic, biochemistry and organometallic research owing to their reactivity and applications in areas such as catalysis, materials science, etc. [1].

Besides, polyhydride complexes of high co-ordination number are subject of considerable attention because of their structural properties, fluxional behaviour, and the possibility of containing non-classical η^2-H_2 ligands [2]. The stability of these non-classical structures depends on both electronic and steric factors, and the ancillary ligands can play an important role in this stabilisation [3].

Although a large number of rhenium polyhydride phosphine complexes are known, there are a few examples in which phosphite or *mixed phosphite* species [$PR_n(OR)_{3-n}$; $n = 0–2$] have been used as ancillary ligands and the majority of them are monodentate ligands [4]. The weaker σ-donor and stronger π-acceptor properties of these ligands as compared to phosphines [5] should influence the properties of the metal centre and that is why we have focused our research interest in studying rhenium polyhydride complexes in which phosphites or *mixed phosphites* with different denticity are used as co-ligands. In this paper we report the characterisation of several pentahydride rhenium complexes with mixed bidentate and monodentate phosphites as ancillary ligands. X-ray structures, variable-temperature NMR and protonation studies are also presented.

2. Results and discussion

2.1. Synthesis

Complexes $[ReCl_3L^1\{P(OMe)_3\}]$ (**1a**) and $[ReCl_3L^1\{P(OEt)_3\}]$ (**1b**), (L^1 = 1,2-bis(diphenylphosphinite)ethane) were synthesised by reacting the oxochloride

* Corresponding author. Tel.: +34-986812275; fax: +34-986813798.
E-mail address: jbravo@uvigo.es (J. Bravo).

0022-328X/02/$ - see front matter © 2002 Elsevier Science B.V. All rights reserved.
doi:10.1016/S0022-328X(02)02151-4

$[ReOCl_3L^1]$ with the appropriate *phosphite* ligands following the procedure previously described [4b]. The yellow paramagnetic air-stable solids obtained were characterised by elemental analysis. ^{1}H-NMR spectra show that proton resonances are paramagnetically shifted (Section 4).

Reaction of complexes **1a** and **1b** with $NaBH_4$ yielded the pentahydrides $[ReH_5L^1\{P(OMe)_3\}]$ (**2a**) and $[ReH_5L^1\{P(OEt)_3\}]$ (**2b**). Air-stable crystals of both compounds suitable for a single-crystal X-ray structure analysis were grown in methanol and ethanol solutions, respectively.

In order to investigate the influence of ancillary ligands on the properties of the pentahydrides we have also synthesised the compounds $[ReH_5L^1L^2]$ (**2**; $L^2 =$ $PPh(OMe)_2$ (**c**), $PPh(OEt)_2$ (**d**), $PPh_2(OMe)$ (**e**), $PPh_2(OEt)$ (**f**)), about which we had already reported some preliminary results [6].

2.2. Variable-temperature NMR spectra

Complexes **2a**–**f** show high fluxionality at all accessible temperatures (>174 K) but this behaviour varies significantly with the nature of the monodentate auxiliary ligand (L^2).

All the compounds show, at room temperature, a typical AX_2 ^{31}P-NMR spectrum with a triplet assignable to L^2, and a doublet corresponding to the bidentate ligand L^1, indicating the magnetic equivalence of their P nuclei due to the fluxionality of the molecule at that temperature. As the temperature decreases the triplet converts into a broad double doublet and the doublet into two broad signals (a double doublet and a singlet). Compound **2e** is an exception: at room temperature it behaves as an AB_2 system (due to the similarity of the surroundings of the phosphorus atoms in both ligands) with the signals collapsing to a broad singlet when the temperature is lowered.

In the room temperature ^{1}H-NMR spectra of the compounds the signal of the five-hydride ligands appears as a double triplet owing to their fluxionality and to the different coupling with the phosphorus nuclei of the two ligands. The chemical shift of this signal is influenced by the electron-withdrawing character of the substituents on L^2, shifting from a value of -6.68 ppm for complex **2a** to -5.95 ppm for **2f**. In the decoupled $^1H\{^{31}P\}$ NMR spectra these signals appear as singlets showing no evidence of H–H coupling (see, e.g. Fig. 1b).

On cooling the sample, the hydride signal broadens and two or three coalescence events (depending on the number of OR groups of L^2) can be observed. In Figs. 1 and 2 we present the temperature variable spectra shown by complexes **2b** and **2e** (having three and one OR groups, respectively) for hydride resonances. At 183 K the spectrum of **2e** (Fig. 2) shows three resonances at -5.59, -6.11 and -6.47 ppm integrating to 1:1:3 protons, respectively. By contrast, the spectrum of **2b** presents, at 174 K, two better resolved signals, the first centred at -5.77 and the second at -7.12 ppm,

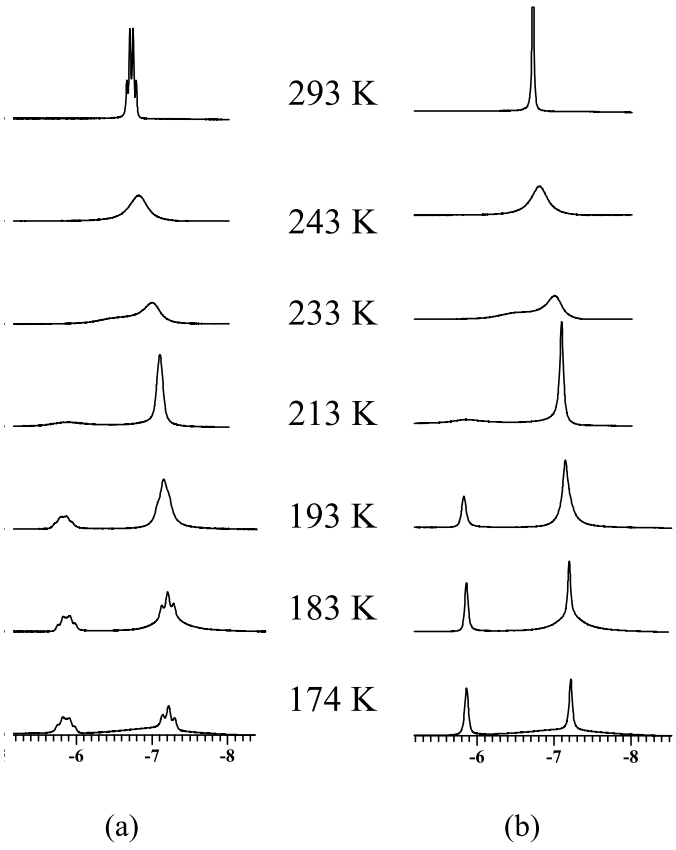

Fig. 1. Variable-temperature 400 MHz ^{1}H (a) and $^1H\{^{31}P\}$ (b) NMR spectra in the hydride region of $[ReH_5L^1\{P(OEt)_3\}]$ (**2b**) in CD_2C1_2.

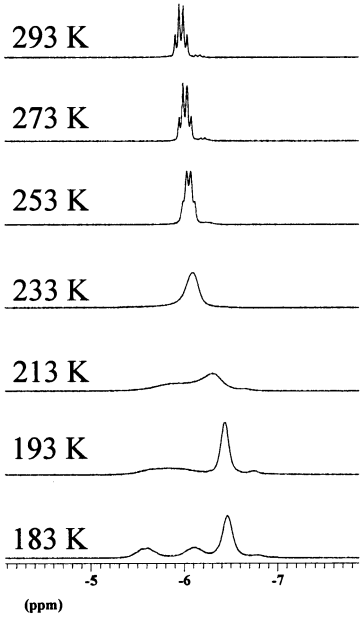

Fig. 2. Variable-temperature 400 MHz ^{1}H-NMR spectra in the hydride region of $[ReH_5L^1\{PPh_2(OMe)\}]$ (**2e**) in CD_2C1_2. A small peak at ca. -6.8 ppm at 183 K is an impurity.

integrating to 1:1 protons, and one more signal (at −7.1 ppm), almost buried in the baseline as a result of a decoalescence process involving the other three protons (Fig. 1).

When temperature is raised we can see two more coalescence events for both compounds. The first one involves the two protons not included in the previous process and produces a coalescence signal at around 213 K for compound **2e** and at 233 K for **2b**. Finally, a broad signal arises, integrating for five protons (at 233 K for **2e** and 243 for **2b**), as a result of a higher temperature coalescence process. In summary, the compounds become more rigid as the number of OR groups on L^2 increases (Fig. 3). The nature of the R group (Me or Et) does not seem to have a significative influence on this behaviour.

With the aim of proposing a mechanism for the different exchange processes observed, we have carried out a kinetic study using a NMR spectral simulation software [7]. Since all our systems are very fluxional and we could not obtain the static spectra, the lineshape NMR signal analysis in not very reliable, but we have made an estimation for one of the more rigid complexes (**2b**). Fig. 4 shows the Eyring plots for the two highest temperature exchange processes with the values of $\Delta H^{\ddagger}$ obtained. These values are similar to those reported for other rhenium pentahydrides [8]. The lowest temperature exchange is too fast to be evaluated, but it could be tentatively assigned to a turnstile rotation of the three H's (H1, H2 and H5 in Fig. 6) situated on a triangular face of the dodecahedron (see 'a' in Scheme 1). This mechanism was also proposed by Crabtree et al. for $[ReH_5(PPh_3)_2(py)]$ [8]. The second exchange on warming involves the two other protons and may be a pairwise exchange between H3 and H4 (see 'b' in Scheme 1).

Finally, a pseudorotation H1–H4 analogous to the Crabtree's proposal (Scheme 2) that causes all the hydrides to exchange could be a likely one.

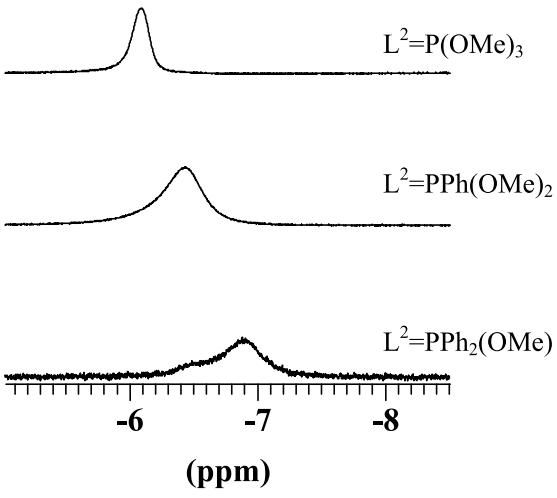

Fig. 3. Hydride signal of compounds **2a**, **2c** and **2e** at 193 K.

Longitudinal $T_{1(min)}$ relaxation times were determined for the hydride signals of the compounds at 400 MHz using the standard inversion-recovery method. All the compounds show a well-defined 'V-shaped' plot of ln T_1 against $1/T$, and similar values of $T_{1(min)}$ between 116 and 127 ms (Table 1) which indicates the classical nature of the hydrides [9]. A relationship between those values and the different nature of L^2 can not be established.

We have also carried out a calculation of relaxation rates of the hydride ligands (R_{cal}) for compound **2b** using the structural data obtained for these compounds by X-ray crystallography and following the criteria indicate by Halpern et al. [9b]. The calculated $T_{1(min)}$ is in good agreement with the experimental value, providing an extra reliability to the structural parameters obtained from the X-ray analysis.

Relaxation rates were obtained by summing the contributions of the interactions of the hydride ligands with the other hydrides ($R_{H-H(m)}$), the rhenium (R_{H-Re}) and the phosphorous (R_{H-P}) nuclei, the *ortho* hydrogens of the phenyl rings ($R_{H-H(ortho)}$) and the methylene ($R_{H-H(CH_2)}$) and methyl ($R_{H-H(CH_3)}$) hydrogens of the L^1 and L^2 ligands:

$$R_{cal} = R_{H-H(m)} + R_{H-Re} + R_{H-P} + R_{H-H(ortho)} + R_{H-H(CH_2)} + R_{H-H(CH_3)}$$

$R_{cal} = 3.160\ s^{-1} + 1.976\ s^{-1} + 0.104\ s^{-1} + 0.614\ s^{-1} + 0.511\ s^{-1} + 0.033\ s^{-1} = 6.398\ s^{-1}$ that corresponds to a T_1 value of 125 ms at 400 MHz (the experimental value was 116 ± 12 ms).

2.3. Description of the structures

Figs. 5 and 6 show the view of the compounds together with the atomic numbering scheme. Selected bond lengths and angles with the estimated deviations are listed in Table 2.

The compounds have an eight co-ordination core, formed by the five hydride ligands and three phosphorus atoms. There are no significant interactions between the molecules.

The presence of different monodentate phosphite ligands in the co-ordination sphere of the rhenium atom produces some changes in the molecule but they do not affect the co-ordination core, which is best described as a distorted dodecahedron. A view of the co-ordination polyhedron is also shown in the figures. The L^1 and L^2 ligands and one of the hydride ligands (labelled as H5) occupy the B sites. The four other hydride ligands are in the A sites [10] (Scheme 3).

The dodecahedral co-ordination geometry can be seen as two orthogonal trapezoidal planes. One of these planes is formed by the phosphorus atom of the monodentate ligand (labelled as P1), one of the phosphorus atoms of the bidentate ligand (P2), and two

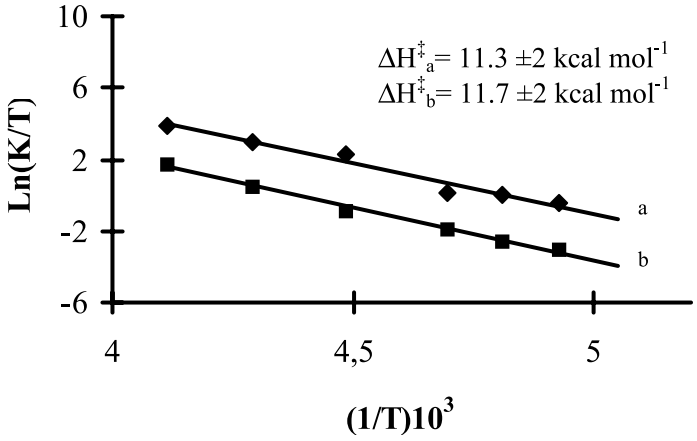

Fig. 4. Eyring plots for the highest (b) and intermediate (a) temperature proton exchange in **2b**.

hydride ligands (H1 and H2). The rhenium atom is located out of this plane by 0.248(12) and 0.204(11) Å for **2a** and **2b**, respectively. Hydride ligands H3, H4, H5 and the remaining phosphorus atom of the bidentate ligand form the other trapezoidal plane, with dihedral angles of 89.8(15)° in both compounds. These planes practically contain the rhenium atom (at 0.038(40) and 0.025(20) Å, respectively) and each one of them can be considered as a mirror plane in the metal core.

On the other hand, the rhenium atom is 0.3888(15) and 0.3937(6) Å out of the plane formed by the three phosphorus atoms. Hydride atoms labelled as H1, H2 and H5 are located at one side and H3 and H4 at the other side of the plane.

Two of the three Re–P bond lengths are very similar to each other in both complexes, being the third one slightly shorter. As expected, the shortest Re–P bond length corresponds to the monodentate ligand possibly due the electron-withdrawing substituents on the P atom which increase the 's' character of the Re–P bond [5].

For compound **2b** the geometrical parameters of the Re–H bond lengths and angles are set out in Table 2. The Re–H bond lengths have values in the range 1.56(2)–1.66(5) (average 1.61(6) Å) Å. The H···H interatomic distances are in accordance with the presence of only classical hydrides around the rhenium atom.

The P1–Re–P2 bond angles are broader (151.42(8)° and 151.61(3)° for **2a** and **2b**, respectively) than P1–Re–P3 and P2–Re–P3 angles (average 98.64(5)°), giving the characteristic two angle types for this kind of compounds [10].

Unfortunately, for compound **2a** the geometrical parameters of the Re–H bond lengths and angles are not trustworthy since some restrains were applied during the refinement due to the poorer quality of the crystal data, but they are in good agreement with those found in similar complexes.

Crystallographic data for the structural analysis have been deposited with the Cambridge Crystallographic

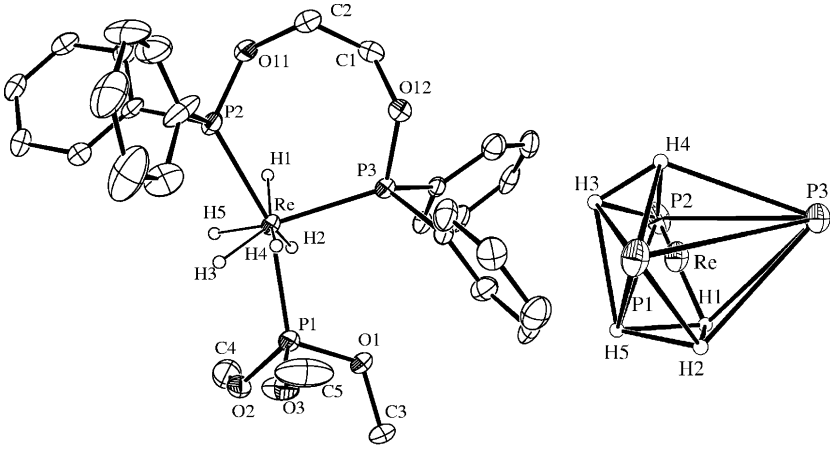

Fig. 5. Molecular diagram and rhenium core for $[ReH_5L^1\{P(OMe)_3\}]$ (**2a**).

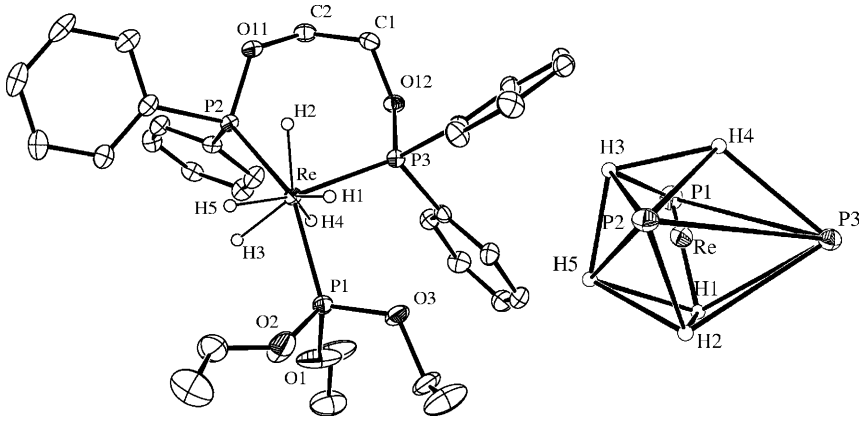

Fig. 6. Molecular diagram and rhenium core for $[ReH_5L^1\{P(OEt)_3\}]$ (**2b**).

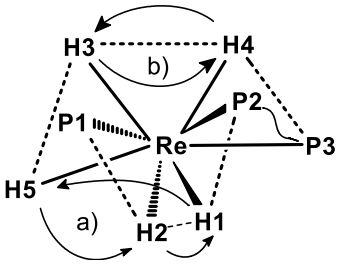

Scheme 1.

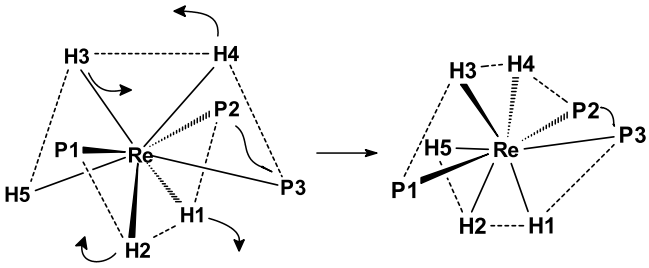

Scheme 2.

Table 1
$T_{1(min)}$ data at 400 MHz for compounds **2a**–**f**

Compound		T/K	T_1/ms
2a	$[ReH_5L^1\{P(OMe)_3\}]$	222	121±12
2b	$[ReH_5L^1\{P(OEt)_3\}]$	224	116±12
2c	$[ReH_5L^1\{PPh(OMe)_2\}]$	224	112±11
2d	$[ReH_5L^1\{PPh(OEt)_2\}]$	225	115±10
2e	$[ReH_5L^1\{PPh_2(OMe)\}]$	226	124±10
2f	$[ReH_5L^1\{PPh_2(OEt)\}]$	229	127±10

Data Centre (CCDC) Nos. 189621 and 189622 for compounds **2a** and **2b**, respectively. Copies of this information may be obtained free of charge from the Director, CCDC, 12 Union Road, Cambridge, CB2 1EZ, UK (Fax: +44-1223-336033; e-mail: deposit@ccdc.cam.ac.uk or available from http://www.ccdc.cam.ac.uk.

Table 2
Selected bond lengths (Å) and angles (°) for $[ReH_5L^1\{P(OR)_3\}]$

	$[ReH_5L^1\{P(OMe)_3\}]$	$[ReH_5L^1\{POEt)_3\}]$
Re–P(1)	2.316(2)	2.3166(10)
Re–P(2)	2.361(2)	2.3633(9)
Re–P(3)	2.366(2)	2.3577(9)
Re–H(1)	1.588(19)	1.63(6)
Re–H(2)	1.59(2)	1.66(5)
Re–H(3)	1.59(2)	1.56(5)
Re–H(4)	1.60(2)	1.560(18)
Re–H(5)	1.59(2)	1.64(5)
P(1)–Re–P(2)	151.42(8)	151.61(3)
P(1)–Re–P(3)	98.30(7)	98.54(3)
P(2)–Re–P(3)	99.26(7)	98.46(3)
P(1)–Re–H(3)	68(4)	75.3(17)
P(2)–Re–H(3)	83(4)	76.8(17)
P(3)–Re–H(3)	128(4)	138.3(18)
P(1)–Re–H(5)	92(3)	85.7(15)
P(1)–Re–H(1)	131.5(18)	70.1(18)
P(2)–Re–H(1)	71.7(17)	135.0(19)
P(2)–Re–H(5)	87(3)	89.0(15)
P(3)–Re–H(5)	144(3)	153.7(16)
P(3)–Re–H(1)	88(2)	82(2)
P(1)–Re–H(4)	73(3)	82.1(14)
P(2)–Re–H(4)	87(3)	83.3(14)
P(3)–Re–H(4)	83(3)	68.4(14)
P(1)–Re–H(2)	72.7(18)	134.3(19)
P(2)–Re–H(2)	130.1(18)	69.9(19)
P(3)–Re–H(2)	88(2)	85.0(19)
H(5)–Re–H(1)	61(3)	75(3)
H(3)–Re–H(5)	87(5)	68(2)
H(3)–Re–H(1)	140(4)	131(3)
H(3)–Re–H(4)	46(4)	70(2)
H(5)–Re–H(4)	133(4)	138(2)
H(1)–Re–H(4)	155(3)	135(3)
H(5)–Re–H(2)	62(4)	74(2)
H(1)–Re–H(2)	59.3(10)	65(2)
H(3)–Re–H(2)	129(4)	129(3)
H(4)–Re–H(2)	143(3)	139(2)

2.4. Protonation studies

Pentahydrides **2a**–**e** were protonated, in CD_2Cl_2, with $HBF_4 \cdot Et_2O$ at 183 K in a NMR tube following the

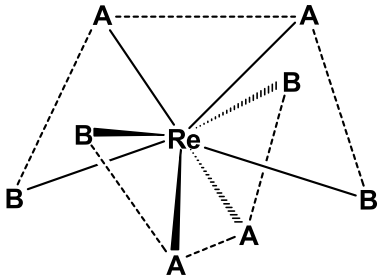

Scheme 3.

procedure giving elsewhere [4c] affording the corresponding dihydrogen complexes **3a**–**e** (Scheme 4).

At 183 K the ^{1}H-NMR spectra of the complexes present a broad singlet between −4 and −5 ppm (Table 3) assignable to the hydride ligands, showing their high fluxionality. The $T_{1(min)}$ values of the compounds are around 20 ms at 400 MHz (Table 3), indicating the presence of a non-classical H_2 ligand. Although this small value could be attributed to the presence of more than one dihydrogen ligand, it must be noted that the rhenium nuclei have an important contribution to the relaxation rates of hydride ligands [9b]. In fact, $T_{1(min)}$ values of 3 and 4 ms (300 MHz) have been reported for cationic complexes $[Re(H_2)(PR_3)_2(CO)_3]^+$ with only one dihydrogen ligand [11].

The singlet converts into a quadruplet ($J_{PH} \sim 12$ Hz) when temperature is raised till 298 K (Fig. 7). This fact is noticeable since dihydrogen complexes usually give a broad signal [2] and a resolved signal is associated with classical hydrides. On the other hand, treatment of these compounds with NEt_3 resulted in the starting pentahydride complexes. A similar behaviour was recently reported for the complexes $[OsX(\eta^2\text{-}H_2)\{PPh(OEt)_2\}_4]BF_4$ (X = Br, I, SEt) but in this case the well resolved signal was already observed at lower temperatures (206–209 K) [12]. This different behaviour may be attributed to the polyhydride nature of our compounds.

Hydride signal disappears gradually in a few hours due to the decomposition of the compounds by losing H_2(g), as we can observe by the appearance of a sharp singlet at 4.63 ppm assignable to free H_2. This signal begins to appear at higher temperature as the number of OR groups on the L^2 ligand increases (253 K for **3e**, 263 K for **3c**, **3d** and 273 K for **3a**, **3b**.). That is, when the electron-withdrawing behaviour of the monodentate phosphite ligand increases, the π-basic character of the metal centre decreases, avoiding an excessive $d(M) \rightarrow \sigma^*(H_2)$ backbonding and stabilising the dihydrogen complex [2b].

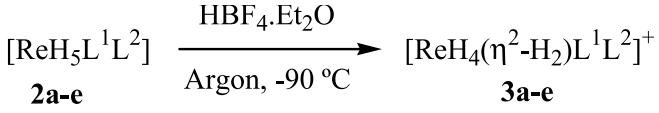

Scheme 4.

The $^{31}P\{^1H\}$ NMR spectra of the complexes show, at 183 K, a triplet corresponding to the monodentate ligand L^2, and a broad hump that corresponds to the phosphorus of bidentate ligand. Raising the temperature this hump converts into a doublet owed to the coupling with the phosphorous atom of L^2 (Table 3).

3. Conclusions

Rhenium pentahydrides $[ReH_5L^1L^2]$, (L^1 = $Ph_2POCH_2CH_2OPPh_2$; $L^2 = PPh_n(OR)_{3-n}$, $n = 0$–2; R = Me, Et) were synthesised by treatment of $[ReCl_3L^1L^2]$ with an excess of $NaBH_4$. Crystal structures of those pentahydrides with $L^2 = P(OR)_3$ show a dodecahedral co-ordination geometry with the three phosphorous donor atoms and one hydride ligand occupying the B sites, and the four other hydride ligands situated at the A sites.

Variable temperature NMR studies show that pentahydrides are of classical nature ($T_{1(min)}$ around 120 ms at 400 MHz) and highly fluxional, becoming more rigid as the number of OR groups of L^2 increases. Three coalescence events can be observed in the more rigid systems and we tentatively suggest turnstile, pairwise and pseudorotation mechanisms for the three processes.

Protonation of pentahydrides with $HBF_4 \cdot Et_2O$, at 183 K, affords dihydrogen complexes as their $T_{1(min)}$ values demonstrate ($\sim$20 ms at 400 MHz). These non-classical compounds lose H_2(g) when the temperature is raised, but the thermal stability increases with the electron-withdrawing character of L^2 probably due to the best tuning between σ-donor and π-acceptor characteristics of the auxiliary phosphorous ligands to provide the critical amount of backbonding from the rhenium centre to the H_2 ligand.

4. Experimental

4.1. General remarks

All operations were carried out in an atmosphere of argon using standard Schlenk techniques. Solvents were purified by distillation from the appropriate drying agents [13] and degassed before use. Elemental analyses were performed on a Fisons EA-1108 apparatus. NMR spectra were collected on a Bruker AMX 400 spectrometer. ^{1}H chemical shifts were measured with the residual solvent resonance as reference and ^{31}P signals to external 85% H_3PO_4, with downfield shifts considered positive. T_1 values were determined by the inversion-recovery method using a standard $180^\circ - \tau - 90^\circ$ pulse sequence. Infrared spectra (IR) of samples in KBr pellets

Table 3
Selected variable temperature NMR data for complexes **3a**–**e**

Compound	^{1}H-NMR [a]			^{31}P{^{1}H} NMR		
	δ (J/Hz) 183 K	δ (J/Hz) 293 K	Assigment	T_1/ms (T/K)	δ (J/Hz) 183 K	δ (J/Hz) 293 K
3a	−4.71 (br)	−4.47 (q)	H/η^2-H_2	21 ± 3	119.0 (br)	117.5 (d)
$[ReH_4(\eta^2\text{-}H_2)L^1\ \{P(OMe)_3\}]^+$		$J_{PH} = 11$		(221)	123.8 (t)	120.8 (t)
		3.36 (d)	CH_3 (L^2)		$J = 48$	$J = 46$
		$J_{PH} = 12$				
		4.11 (m)	$(CH_2)_2$ (L^1)			
3b	−4.58 (br)	−4.39 (q)	H/η^2-H_2	20 ± 5	115.4 (t)	112.5 (t)
$[ReH_4(\eta^2\text{-}H_2)L^1\ \{P(OEt)_3\}]^+$		$J_{PH} = 12$		(206)	118.7 (br)	117.1 (d)
		1.16 (t)	CH_3 (L^2)		$J = 43$	$J = 45$
		3.72 (qnt)	CH_2 (L^2)			
		$J_{PH} = 7$				
		4.13 (m)	$(CH_2)_2$ (L^1)			
3c	−4.20 (br)	−4.20 (q)	H/η^2-H_2	21 ± 4	113.7 (br)	118.4 (d)
$[ReH_4(\eta^2\text{-}H_2)L^1\{PPh(OMe)_2\}]^+$		$J_{PH} = 11$		(228)	126.4 (br)	
		3.28 (d)	CH_3 (L^2)		138.1 (t)	138.9 (t)
		$J_{PH} = 12$			$J = 34$	$J = 35$
		4.09 (m)	$(CH_2)_2$ (L^1)			
3d	−4.28 (br)	−4.15 (q)	H/η^2-H_2	20 ± 2	120.5 (br)	118.3 (d)
$[ReH_4(\eta^2\text{-}H_2)L^1\{PPh(OEt)_2\}]^+$		$J_{PH} = 12$		(231)	130.4 (t)	131.5 (t)
		1.16 (t)	CH_3 (L^2)		$J = 29$	$J = 35$
		3.72 (m)	CH_2 (L^2)			
		4.10 (m)	$(CH_2)_2$ (L^1)			
3e	−4.05 (br)	−3.88 (q)	H/η^2-H_2	21 ± 3	109.0 (t)	111.3 (t)
$[ReH_4(\eta^2\text{-}H_2)L^1\{PPh_2(OMe)\}]^+$		$J_{PH} = 13$		(226)	120.0 (br)	118.3 (d)
		3.11 (d)	CH_3 (L^2)		$J = 23$	$J = 27$
		$J_{PH} = 13$				
		4.11 (m)	$(CH_2)_2$ (L^1)			

In CD_2Cl_2 at 400 MHz.
[a] Phenyl proton resonances are omitted.

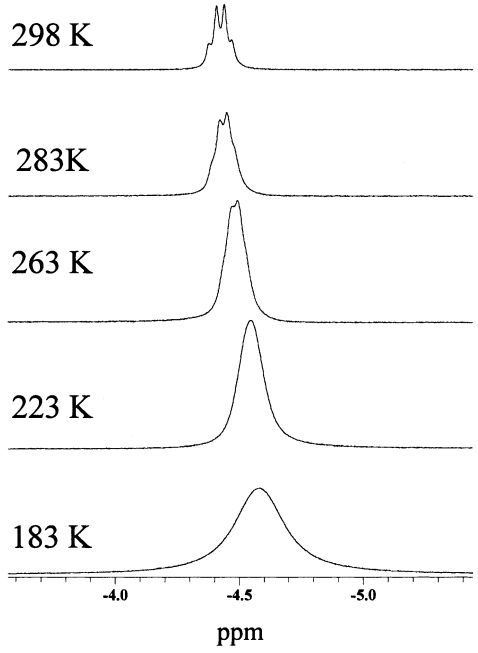

Fig. 7. Variable-temperature 400 MHz ^{1}H-NMR spectra in the hydride region of $[ReH_4(\eta^2\text{-}H_2)L^1\{P(OEt)_3\}]^+$ (**3b**) in CD_2Cl_2.

were recorded on a Bruker Vector IFS28 FT spectrophotometer. The ligand 1,2-bis(diphenylphosphinite)ethane (L^1), $[ReOCl_3L^1]$ and compounds **1c**–**f** were prepared as described previously [6].

4.2. Preparation of $[ReCl_3L^1L^2]$ ($L^2 = P(OMe)_3$ (**1a**), $P(OEt)_3$ (**1b**))

$[ReOCl_3L^1]$ (260 mg, 0.352 mmol for **1a**; 334 mg, 0.452 mmol for **1b**) was dissolved in 30 ml of tetrahydrofuran and an excess (1:3 mol) of the appropriate phosphite was added. The mixture was refluxed for 1 h and stirred for another 3 h. The yellow solution obtained was vacuum concentrated and the resulting oil was taken into methanol (**1a**) or ethanol (**1b**) affording a yellow solid that was filtered out, washed with the same alcohol, and dried under argon.

1a: (0.16 g, 54% yield). ^{1}H-NMR ($CHCl_3$-d_1, 400 MHz, all signals are paramagnetically shifted): $\delta = 17.75$ (4H, Ph), 16.73 (4H, Ph), 11.58 (9H, $-CH_3$), 11.35 (2H, Ph), 10.35 (2H, Ph), 9.14 (4H, $-(CH_2)_2-$), 8.84 (4H, Ph), 8.32 (2H, Ph), 8.20 (2H, Ph) Anal. Found: C, 40.90; H, 4.02. Calc. for $C_{29}H_{33}Cl_3O_5P_3Re$ (847.07): C, 41.12; H, 3.93%.

1b: (0.24 g, 60% yield). ^{1}H-NMR ($CHCl_3$-d_1, 400 MHz, all signals are paramagnetically shifted): $\delta = 17.62$ (4H, Ph), 16.85 (4H, Ph), 11.69 (2H, Ph), 11.28 (6H, $-CH_2-$), 9.70 (2H, Ph), 9.12 (4H, $-(CH_2)_2-$), 8.75 (4H, Ph), 8.32 (2H, Ph), 7.97 (2H, Ph), 2.92 (9H, $-CH_3$). (Anal. Found: C, 43.00; H, 4.51. Calc. for $C_{32}H_{39}Cl_3O_5P_3Re$ (889.15): C, 43.23; H, 4.42%.

4.3. Preparation of $[ReH_5L^1L^2]$ ($L^2 = P(OMe)_3$ (**2a**), $P(OEt)_3$ (**2b**), $PPh(OMe)_2$ (**2c**), $PPh(OEt)_2$ (**2d**), $PPh_2(OMe)$ (**2e**), $PPh_2(OEt)$ (**2f**))

Compounds **2a**, **2c** and **2e** were synthesised as follows: 0.3 g of **1a**, **1c** or **1e** and 0.4 g of $NaBH_4$ were suspended in 40 ml of cold methanol (ca. 233 K) under argon. After 8 h stirring at this temperature, the suspension was allowed to slowly reach room temperature and its colour changed from yellow to brown. The solvent was removed by vacuum and the residue was extracted with 40 ml of benzene. The brown solution obtained was concentrated in vacuo and the resulting product was taken into methanol. The precipitate formed was removed by filtration and the liquid was leaving aside several days obtaining a whitish solid that was filtered out and dried under vacuum.

2a: (0.1 g, 38% yield). IR (KBr pellets, cm^{-1}): υ(Re–H) = 1903 (w), 1927 (w), 1967 (w). ^{1}H-NMR (CH_2Cl_2-d_2, 400 MHz, 293 K): $\delta = -6.68$ [dt, 5H, $J(P_A,H) = 16$ Hz, $J(P_B,H) = 19$ Hz, ReH], 3.23 (d, 9H, $J = 12$ Hz, $-CH_3$), 4.07 [m, 4H, $-(CH_2)_2-$], 7.3–7.9 (m, 20H, Ph). ^{31}P-NMR (CH_2Cl_2-d_2, 161 MHz, 293 K): $\delta = 128.5$ (d, P_A), 150.0 (t, P_B), $J(P_A,P_B) = 57$ Hz. Anal. Found: C, 46.70; H, 5.14. Calc. for $C_{29}H_{38}O_5P_3Re$ (745.75): C, 46.71; H, 5.14%.

2c: (0.08 g, 30% yield). IR (KBr pellets, cm^{-1}): υ(Re–H) = 1907 (w), 1922 (w), 1967 (sh). ^{1}H-NMR (CH_2Cl_2-d_2, 400 MHz, 293 K): $\delta = -6.25$ [dt, 5H, $J(P_A,H) = 16$ Hz, $J(P_B,H) = 18$ Hz, ReH], 3.18 (d, 6H, $J = 12$ Hz, $-CH_3$), 4.05 [m, 4H, $-(CH_2)_2-$], 7.2–7.8 (m, 25H, Ph). ^{31}P-NMR (CH_2Cl_2-d_2, 161 MHz, 293 K): $\delta = 129.7$ (d, P_A), 156.4 (t, P_B), $J(P_A,P_B) = 45$ Hz. Anal. Found: C, 51.65; H, 4.94. Calc. for $C_{34}H_{40}O_4P_3Re$ (791.82): C, 51.57; H, 5.09%.

2e: (0.08 g, 30% yield). IR (KBr pellets, cm^{-1}): υ(Re–H) = 1894 (w), 1931 (w). ^{1}H-NMR (CH_2Cl_2-d_2, 400 MHz, 293 K): $\delta = -5.96$ [dt, 5H, $J(P_A,H) = 16$ Hz, $J(P_B,H) = 19$ Hz, ReH], 3.21 (d, 3H, $J = 13$ Hz, $-CH_3$), 4.03 [m, 4H, $-(CH_2)_2-$], 7.1–7.9 (m, 30H, Ph). ^{31}P-NMR (CH_2Cl_2-d_2, 161 MHz, 293 K): $\delta = 131.0$ (d, P_A), 132.0 (t, P_B), $J(P_A,P_B) = 37$ Hz. Anal. Found: C, 55.60; H, 5.20. Calc. for $C_{39}H_{42}O_3P_3Re$ (837.89): C, 55.91; H, 5.05%.

Compounds **2b** and **2f** were synthesised following the method previously reported for compound **2d** 4b, but starting with 0.3 g of compound **1b** or **1f** and washing the beige solid obtained with ethanol for a longer period of time (2–3 days).

2b: (0.17 g, 64% yield). IR (KBr pellets, cm^{-1}): υ(Re–H) = 1913 (w), 1931 (w), 1970 (sh). ^{1}H-NMR (CH_2Cl_2-d_2, 400 MHz, 293 K): $\delta = -6.60$ [dt, 5H, $J(P_A,H) = 16$ Hz, $J(P_B,H) = 19$ Hz, ReH], 1.09 (t, 9H, J = 7 Hz, $-CH_3$), 3.67 (qnt, 6H, $J = 7$ Hz, $-CH_2-$), 4.09 [m, 4H, $-(CH_2)_2-$], 7.2–7.9 (m, 20H, Ph). ^{31}P-NMR (CH_2Cl_2-d_2, 161 MHz, 293 K): $\delta = 128.8$ (d, P_A), 142.1 (t, P_B), $J(P_A,P_B) = 56$ Hz. Anal. Found: C, 48.60; H, 5.68. Calc. for $C_{32}H_{44}O_5P_3Re$ (787.83): C, 48.79; H, 5.63%.

2f: (0.12 g, 45% yield). IR (KBr pellets, cm^{-1}): υ(Re–H) = 1895 (w), 1935 (w), 1960 (sh). ^{1}H-NMR (CH_2Cl_2-d_2, 400 MHz, 293 K): $\delta = -5.92$ [dt, 5H, $J(P_A,H) = 16$ Hz, $J(P_B,H) = 20$ Hz, ReH], 1.13 (t, 3H, $J = 7$ Hz, $-CH_3$), 3.56 (qnt, 2H, $J = 7$ Hz, $-CH_2-$), 4.04 [m, 4H, $-(CH_2)_2-$], 7.1–7.9 (m, 30H, Ph). ^{31}P-NMR (CH_2Cl_2-d_2, 161 MHz, 293 K): $\delta = 130.8$ (d, P_A), 126.4 (t, P_B), $J(P_A,P_B) = 36$ Hz. Anal. Found: C, 56.60; H, 4.99. Calc. for $C_{40}H_{44}O_3P_3Re$ (851.92): C, 56.40; H, 5.21%.

4.4. Crystal structure determination

The data collections at -100 °C were taken on a SIEMENS Smart CCD area-detector diffractometer with graphite-monochromated Mo–K_α radiation. Absorption corrections were carried out using SADABS [14].

Both structures were solved by direct methods and refined by a full-matrix least-squares based on F^2 [15]. All non-hydrogen atoms were refined with anisotropic displacement parameters. For $[ReH_5L^1\{P(OEt)_3\}]$ the co-ordinated hydrogen atoms were located on difference electron density map and refined with isotropic displacement parameters. For $[ReH_5L^1\{P(OMe)_3\}]$ the poor quality of the crystal data did not allow to locate the co-ordinated hydrogen atoms, but their positions were included with some restrictions on their distances to the rhenium atom. All other hydrogen atoms were placed in calculated positions and refined with a riding model. Atomic scattering factors and anomalous dispersion corrections for all atoms were taken from International Tables for X-ray Crystallography [16]. Details of crystal data and structural refinement are given in Table 4.

Acknowledgements

The financial support from Xunta de Galicia (Project PGIDT-PX130102PR) is gratefully acknowledged. We thank the CACTI NMR and X-ray diffraction services (Universidade de Vigo) for recording NMR spectra and collecting X-ray data.

Table 4
Crystal data and structure refinement

Identification code	**2a**	**2b**
Empirical formula	$C_{29}H_{38}O_5P_3Re$	$C_{32}H_{44}O_5P_3Re$
Formula weight	745.70	787.78
Temperature (K)	173(2)	173(2)
Wavelength (Å)	0.71073	0.71073
Crystal system	Orthorhombic	Monoclinic
Space group	$P2_1nb$	$P2_1/c$
Unit cell dimensions	$a = 8.8784(15)$ Å $b = 12.433(2)$ Å $c = 27.861(5)$ Å	$a = 12.5778(7)$ Å $b = 9.1414(5)$ Å $c = 28.9167(17)$ Å $\beta = 92.6420(10)^\circ$
Volume (Å^3)	3075.4(9)	3321.3(3)
Z	4	4
Absorption coefficient (mm^{-1})	4.142	3.840
Crystal description/colour	Block/colourless	Irregular/colourless
Crystal size (mm)	$0.40 \times 0.10 \times 0.09$	$0.35 \times 0.26 \times 0.25$
Theta range for data collection (°)	1.46–28.01	1.41–28.03
Index ranges	$-11 \le h \le 11$ $-16 \le k \le 13$ $-31 \le l \le 36$	$-14 \le h \le 16$ $-8 \le k \le 12$ $-36 \le l \le 38$
Reflections collected	18 774	20 329
Independent reflections	7148 ($R_{int} = 0.0553$)	7827 ($R_{int} = 0.0318$)
Completeness to theta	99.1%	91.7%
Max/min transmission	1.000 and 0.709	1.000 and 0.773
Data/restraints/parameters	7148/7/366	7827/1/394
Goodness-of-fit on F^2	0.930	1.048
Final R indices ($I > 2\sigma(I)$)	$R_1 = 0.0405$, $wR_2 = 0.0772$	$R_1 = 0.0300$, $wR_2 = 0.0662$
R indices (all data)	$R_1 = 0.0699$, $wR_2 = 0.0836$	$R_1 = 0.0396$, $wR_2 = 0.0688$
Largest diff. peak and hole (eÅ^{-3})	1.030 and −0.798	1.384 and −1.026

References

[1] M. Peruzzini, R. Poli (Eds.), Recent Advances in Hydride Chemistry, Elsevier, Amsterdam, 2001.

[2] (a) G.G. Hlatky, R.H. Crabtree, Coord. Chem. Rev. 65 (1985) 1; (b) P.G. Jessop, R.H. Morris, Coord. Chem. Rev. 121 (1992) 155; (c) D.M. Heinekey, W.J. Oldham, Jr., Chem. Rev. 93 (1993) 913; (d) F. Maseras, A. Lledós, E. Clot, O. Eisenstein, Chem. Rev. 100 (2000) 601.

[3] (a) G.J. Kubas, Acc. Chem. Res. 21 (1988) 120; (b) R.H. Crabtree, Acc. Chem. Res. 23 (1990) 95; (c) R.H. Crabtree, Angew. Chem. Int. Ed. Engl. 32 (1993) 789; (d) R.H. Morris, Can. J. Chem. 74 (1996) 1907; (e) N. Mathew, B.R. Jagirdar, R.S. Gopalan, G.U. Kulkarni, Organometallics 19 (2000) 4506.

[4] (a) M. Freni, P. Romiti, Inorg. Nucl. Chem. Lett. 6 (1970) 167; (b) L.F. Rhodes, K.G. Caulton, W.K. Rybak, J.J. Ziolkowski, Polyhedron 5 (1986) 1891; (c) S. García-Fontán, A. Marchi, L. Marvelli, R. Rossi, S. Antoniutti, G. Albertin, J. Chem. Soc. Dalton Trans. (1996) 2779.

[5] C.A. Tolman, Chem. Rev. 77 (1977) 313.

[6] S. Bolaño, J. Bravo, S. García-Fontán, Inorg. Chim. Acta 315 (2001) 81.

[7] P.H.M. Budzelaar, gNMR Version 4.1, Cherwell Scientific Limited, Oxford, 1999.

[8] (a) J.C. Lee, Jr., W. Yao, R.H. Crabtree, H. Rüegger, Inorg. Chem. 35 (1996) 695; (b) R. Bosque, F. Maseras, O. Eisenstein, B.P. Patel, W. Yao, R.H. Crabtree, Inorg. Chem. 36 (1997) 5505.

[9] (a) M.T. Bautista, K.A. Earl, P.A. Maltby, R.H. Morris, C.T. Schweiter, A. Sella, J. Am. Chem. Soc. 110 (1988) 7031; (b) P.J. Desrosiers, L. Cai, Z. Lin, R. Richards, J. Halpern, J. Am. Chem. Soc. 113 (1991) 4173.

[10] (a) T.J. Emge, T.F. Koetzle, J.W. Bruno, K.G. Caulton, Inorg. Chem. 23 (1984) 4012; (b) Y. Kim, H. Deng, J.C. Galluci, A. Woycicki, Inorg. Chem. 35 (1996) 7166.

[11] D.M. Heinekey, B.M. Schomber, C.E. Radzewich, J. Am. Chem. Soc. 116 (1994) 4515.

[12] G. Albertin, S. Antoniutti, E. Bordignon, M. Pegoraro, J. Chem. Soc. Dalton Trans. (2000) 3575.

[13] D.D. Perrin, W.L.F. Armarego (Eds.), Purification of Laboratory Chemicals, third ed., Butterworth and Heinemann, Oxford, 1988.

[14] G.M. Sheldrick, SADABS, an Empirical Absorption Correction Program for Area Detector Data, University of Göttingen, Germany, 1996.

[15] G.M. Sheldrick, SHELX-97, Program for the Solution and Refinement of Crystal Structures, University of Göttingen, Germany, 1997.

[16] International Tables for X-ray Crystallography, vol. C, Kluwer, Dordrecht, 1992.